



Functional model for catecholase-like activity: A mechanistic approach with manganese(III) complexes of salen type Schiff base ligands

Piya Seth^{a,1}, Michael G.B. Drew^b, Ashutosh Ghosh^{a,*}

^a Department of Chemistry, University College of Science, University of Calcutta, 92, A.P.C. Road, Kolkata 700009, India

^b School of Chemistry, The University of Reading, P.O. Box 224, Whiteknights, Reading RG6 6AD, UK

ARTICLE INFO

Article history:

Received 3 April 2012

Received in revised form 23 August 2012

Accepted 25 August 2012

Available online 1 September 2012

Keywords:

Manganese(III)

Schiff base

Crystal structure

Catecholase activity

ABSTRACT

Three new Mn(III) complexes $[\text{MnL}^1(\text{OOCH})(\text{OH}_2)]$ (**1**), $[\text{MnL}^2(\text{OH}_2)_2][\text{Mn}_2\text{L}_2^2(\text{NO}_2)_3]$ (**2**) and $[\text{Mn}_2\text{L}_2^1(\text{NO}_2)_2]$ (**3**) (where $\text{H}_2\text{L}^1 = \text{H}_2\text{Me}_2\text{Salen} = 2,7\text{-bis}(2\text{-hydroxyphenyl})\text{-}2,6\text{-diazaocta-}2,6\text{-diene}$ and $\text{H}_2\text{L}^2 = \text{H}_2\text{Salpn} = 1,7\text{-bis}(2\text{-hydroxyphenyl})\text{-}2,6\text{-diazasepta-}1,6\text{-diene}$) have been synthesized. X-ray crystal structure analysis reveals that **1** is a mononuclear species whereas **2** contains a mononuclear cationic and a dinuclear nitrite bridged ($\mu\text{-}1\kappa\text{O:}2\kappa\text{O}'$) anionic unit. Complex **3** is a phenoxido bridged dimer containing terminally coordinated nitrite. Complexes **1–3** show excellent catecholase-like activity with 3,5-di-*tert*-butylcatechol (3,5-DTBC) as the substrate. Kinetic measurements suggest that the rate of catechol oxidation follows saturation kinetics with respect to the substrate and first order kinetics with respect to the catalyst. Formation of bis($\mu\text{-oxo}$)dimanganese(III,III) as an intermediate during the course of reaction is identified from ESI-MS spectra. The characteristic six line EPR spectra of complex **2** in the presence of 3,5-DTBC supports the formation of manganese(II)-semiquinone as an intermediate species during the catalytic oxidation of 3,5-DTBC.

© 2012 Elsevier B.V. All rights reserved.

1. Introduction

Metalloenzymes that activate molecular oxygen have received great attention as potential catalysts for specific oxidation reactions and also for the development of efficient small molecule catalysts [1–6]. The oxidation of organic substrates with molecular oxygen under mild conditions is of growing interest for industrial and synthetic processes [7]. As a result synthesis and reactivity studies of transition metal complexes, as model compounds for metalloenzymes with oxidase activity have been undertaken by various groups in order to develop bio-inspired catalysts for oxidation reactions [8–10]. One of the major enzymes that play a key role in these reactions is catechol oxidase (CO), a lesser known member of the type-III copper proteins. This enzyme belongs to the polyphenol oxidases which oxidize phenolic compounds to the corresponding quinones in the presence of oxygen. Quinones are highly reactive compounds that autopolymerize to brown polyphenolic catechol melanins. Some higher plants utilize this process to resist diseases and to protect themselves from pathogens or insects.

Most abundant functional mimics of CO are mono- or dinuclear Cu(II) complexes [9,10] as the native form of this enzyme

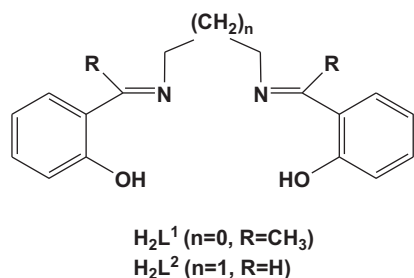
consists of a hydroxo-bridged dicopper(II) center. Therefore, structure–activity relationships for the catechol oxidation reaction are mainly investigated with Cu(II) complexes [11]. From this survey, it can be said that the rate of catechol oxidation reactions catalyzed by Cu(II) complexes is a composite effect of several parameters such as: M–M distance, flexibility of the ligand, type of exogenous ligand and coordination geometry around the metal ion. Besides the Cu(II) containing species, some complexes of Mn(II) [12–14], Mn(III) [15,16], Mn(IV) [17,18] have also been reported to perform catecholase mimicking activity. In these complexes different types of ligands e.g. tetra-dentate tripodal ligands, several pyridine derivatives, azametallacrown and compartmental ligands have been utilized. However, the number of such studies is far less in comparison to Cu(II) complexes, although the manganese(III) complexes play very important roles in biological systems e.g. in many metalloenzymes, redox and non-redox proteins [19,20], and are used as catalysts in olefin epoxidation reactions [21].

In order to have clearer insight into the catecholase activity of manganese complexes we have chosen complexes of salen-type Schiff base ligands (Scheme 1), and synthesized three new Mn(III) complexes, $[\text{MnL}^1(\text{OOCH})(\text{OH}_2)]$ (**1**), $[\text{MnL}^2(\text{OH}_2)_2][\text{Mn}_2\text{L}_2^2(\text{NO}_2)_3]$ (**2**) and $[\text{Mn}_2\text{L}_2^1(\text{NO}_2)_2]$ (**3**). Their characterization, crystal structure and catecholase activity are reported in this paper. All three complexes exhibit substantial catechol oxidation with 3,5-di-*tert*-butylcatechol (3,5-DTBC) as the substrate in acetonitrile solvent. The phenoxido bridged dinuclear

* Corresponding author. Tel.: +91 9433344484; fax: +91 3323519755.

E-mail address: ghosh.59@yahoo.com (A. Ghosh).

¹ Tel.: +91 9433344484; fax: +91 33 2351 9755.



Scheme 1. Schiff base ligand H_2L .

Mn(III) compounds with this kind of N_2O_2 donor Schiff base ligands are well known for their interesting magnetic properties [22] specially for their potential use as single molecule magnets [23]. A nitrito bridged complex of such ligand also exhibited the sign of SMM behavior [24]. However, the catecholase activity of Mn(III) complexes with salen type di-Schiff bases have not been explored till date. We show here that these complexes are very good catalysts for catechol oxidation reaction and try to explain the plausible mechanisms for the same. A manganese(II)-semiquinonate intermediate which is identified through EPR measurements is thought to be responsible for this oxygenation reaction. ESI-MS positive spectra also signify the presence of a bis(μ -oxo)dimanganese(III,III) intermediate during the aerobic oxidation of catechol.

2. Experimental

2.1. Synthesis of the complexes

o-Hydroxy acetophenone, 1,2-ethanediamine, salicylaldehyde and 1,3-diaminopropane were purchased from Lancaster and were of reagent grade. They were used without further purification.

2.1.1. Synthesis of the Schiff base ligands, H_2L^1 and H_2L^2

The two di-Schiff-base ligands, H_2L^1 and H_2L^2 (Scheme 1), were prepared by standard methods [25]. Briefly, 2 mM of diamine {1,2-ethanediamine (0.12 mL) or 1,3-diaminopropane (0.16 mL)} was mixed with 4 mM of the required aldehyde {*o*-hydroxy acetophenone (0.48 mL) or salicylaldehyde (0.41 mL)} in methanol solvent. The resulting mixture was refluxed for ~1.5 h, and allowed to cool. The yellow solutions were used directly for complex formation.

2.1.2. Synthesis of complex $[\text{MnL}^1(\text{OOCH})(\text{OH}_2)](\mathbf{1})$

A methanolic solution (10 mL) of H_2L^1 (2 mM) was added to a methanolic solution (5 mL) of $\text{Mn}(\text{ClO}_4)_2 \cdot 6\text{H}_2\text{O}$ (0.722 g, 2 mM) with constant stirring. After ~10 min an aqueous solution of HCOONa (0.136 g, 2 mM) was added to the solution, followed by triethyl amine (0.56 mL, 4 mM). The solution was further stirred for half an hour. A dark brown crystalline compound separated on stirring. It was filtered. On slow evaporation of the solvent from the filtrate dark brown, X-ray quality single crystals were obtained.

Complex 1: Yield: 0.313 g (78%) Anal. Calc. for $\text{C}_{19}\text{H}_{21}\text{Mn}_1\text{N}_2\text{O}_5$: C, 55.35; H, 5.13; N, 6.79; Found: C, 55.47; H, 5.07; N, 6.62. IR (KBr pellet): $\nu(\text{C}=\text{N})$, 1590 cm^{-1} , $\nu_{\text{as}}(\text{C}=\text{O})$, 1537 cm^{-1} , $\nu_{\text{s}}(\text{C}=\text{O})$, 1328 cm^{-1} . UV-vis (CH_3CN) λ_{max} (nm), $\epsilon(\text{M}^{-1}\text{cm}^{-1})$: 396 (9491).

2.1.3. Synthesis of the complexes $[\text{MnL}^2(\text{OH}_2)_2][\text{Mn}_2\text{L}_2^2(\text{NO}_2)_3]$ (**2**) and $[\text{Mn}_2\text{L}_2^1(\text{NO}_2)_2]$ (**3**)

A methanolic solution (10 mL) of the required ligand H_2L^1 or H_2L^2 (2 mM) was added to a methanolic solution 5 mL of $\text{MnCl}_2 \cdot 4\text{H}_2\text{O}$ (0.394 g, 2 mM) with constant stirring. To this solution triethylamine (0.56 mL, 4 mM) was added. After ca. 15 min a H_2O -MeOH mixture of NaNO_2 (0.169 g, 2 mM) was added to the mixture and stirred. The dark brown compound of both **2** and **3**

started to separate on stirring; the solids were filtered after about 2 h and washed with diethyl ether, and then redissolved in CH_3CN . Layering of these brown solutions with Et_2O gave well formed X-ray quality single crystals.

Complex 2: Yield: 0.846 g (72%) Anal. Calc. for $\text{C}_{51}\text{H}_{52}\text{Cl}_{0.38}\text{Mn}_3\text{N}_{8.62}\text{O}_{13.23}$: C, 51.92; H, 4.44; N, 10.68; Found: C, 51.76; H, 4.31; N, 10.51. IR (KBr pellet): $\nu(\text{C}=\text{N})$, 1612 cm^{-1} , $\nu_{\text{s}}(\text{NO}_2)$, 1295 cm^{-1} , $\nu_{\text{as}}(\text{NO}_2)$, 1213 cm^{-1} , $\nu(\text{H}_2\text{O})$, 3395 cm^{-1} . UV-vis (CH_3CN) λ_{max} (nm), $\epsilon(\text{M}^{-1}\text{cm}^{-1})$: 388 (17,549).

Complex 3: Yield: 0.584 g (75%) Anal. Calc. for $\text{C}_{36}\text{H}_{36}\text{Cl}_{1.02}\text{Mn}_2\text{N}_{4.98}\text{O}_{5.96}$: C, 54.69; H, 4.59; N, 10.63; Found: C, 54.52; H, 4.69; N, 10.47. IR (KBr pellet): $\nu(\text{C}=\text{N})$, 1589 cm^{-1} , $\nu_{\text{s}}(\text{NO}_2)$, 1313 cm^{-1} , $\nu_{\text{as}}(\text{NO}_2)$, 1234 cm^{-1} . UV-vis (CH_3CN) λ_{max} (nm), $\epsilon(\text{M}^{-1}\text{cm}^{-1})$: 397 (9013).

2.2. Physical measurements

Elemental analyses (carbon, hydrogen and nitrogen) were performed using a Perkin-Elmer 240C elemental analyzer. IR spectra in KBr (4000–500 cm^{-1}) were recorded using a Perkin-Elmer RXI FT-IR spectrophotometer. Electronic spectra in acetonitrile (600–300 nm) were recorded in a Hitachi U-3501 spectrophotometer. The electro spray ionization mass (ESI-MS positive) spectra were recorded on a MICROMASS Q-TOF mass spectrometer. The X-band (9.1 GHz) EPR spectra were recorded using a JEOL JES-FA 200 instrument at liquid nitrogen temperature (77 K) in acetonitrile solvent.

2.2.1. Catalytic oxidation of 3,5-DTBC

In order to examine the catecholase activity of the complexes, a 10^{-5} M solution of **1–3** in acetonitrile solvent was treated with 100 equiv. of 3,5-di-*tert*-butylcatechol (3,5-DTBC) under aerobic conditions at room temperature. Absorbance vs. wavelength (wavelength scans) of these solutions were recorded at a regular time interval of 5 min in the wavelength range 300–500 nm. To determine the dependence of rate on substrate concentration and various kinetic parameters, a 10^{-5} M solution of these complexes was treated with at least 10 equiv. of substrate so as to maintain the pseudo first order condition. The reaction was followed spectrophotometrically by monitoring the increase in the absorbance at 400 nm (Quinone band maxima) as a function of time (time scan).

2.3. Crystallographic data collection and refinement

Crystal data for the three complexes **1–3** are given in the supporting information, Table ST1. 4021, 14044 independent reflections data were collected with $\text{MoK}\alpha$ radiation for **1** and **2** at 150 K using the Oxford Diffraction X-Calibur CCD System. The crystals were positioned at 50 mm from the CCD. 321 frames were measured with a counting time of 10 s. Data analyses were carried out with the CrysAlis program [26]. 2556 independent reflections data for **3** were collected with $\text{MoK}\alpha$ radiation at room temperature using the Bruker-AXS SMART APEX II diffractometer equipped with a graphite monochromator and $\text{MoK}\alpha$ ($\lambda = 0.71073 \text{ \AA}$) radiation. The crystal was positioned at 60 mm from the CCD. 360 frames were measured with a counting time of 10 s. All three structures were solved using direct methods with the Shelxs97 program [27]. Both **2** and **3** showed some disorder between one terminal nitrite and chloride ions. In **2** this was treated via population parameters x and $1-x$, respectively with x refined to 0.62(1). In **3** similar refinement converged to 0.49(3) and was subsequently fixed at 0.5. The non-hydrogen atoms were refined with anisotropic thermal parameters. The hydrogen atoms bonded to carbon were included in geometric positions and given thermal parameters equivalent to 1.2 times (or 1.5 times for methyl groups) those of the atom to which they were attached. The hydrogen atoms of the water molecules in **1** and

2 were located in difference Fourier maps and refined with distance constraints. Absorption corrections were carried out using the ABSPACK program [28] for **1** and **2** and the SADABS program for **3** [29]. The structures were refined on F^2 to $R1$ 0.0756, 0.0909, 0.1061; $wR2$ 0.1968, 0.1850, 0.3331 for 2903, 6142, 2126 data with $I > 2\sigma(I)$.

3. Results and discussion

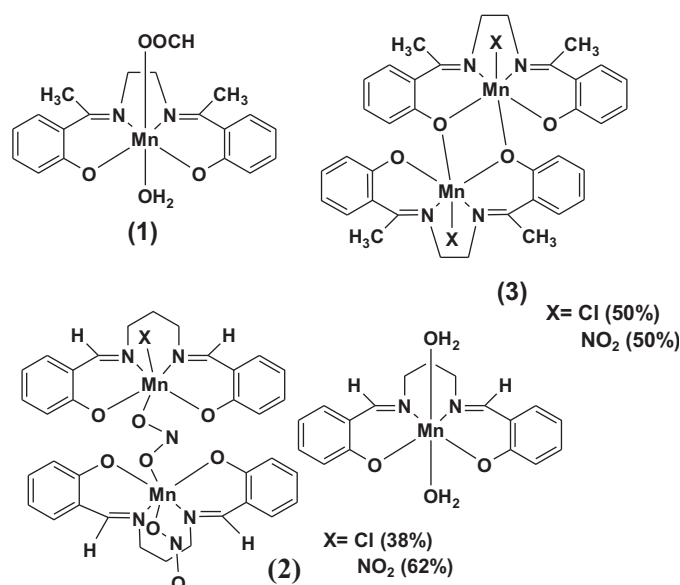
3.1. Syntheses, IR and UV-vis spectra of the complexes

Compound **1** was synthesized by the reaction of H_2L^1 , $Mn(ClO_4)_2 \cdot 6H_2O$, $HCOONa$, Et_3N in 1:1:1:2 molar ratio in methanol solvent. Compounds **2** and **3** were synthesized by the similar reaction of H_2L^1 or H_2L^2 , $MnCl_2 \cdot 4H_2O$, $NaNO_2$ and triethylamine in 1:1:1:2 molar ratios using H_2O – $MeOH$ (1:10) as solvent. The Mn(II) ion was oxidized by the aerial oxygen to Mn(III) under the reaction conditions and the donor atoms of the deprotonated ligand (H_2L) coordinate to form the equatorial plane of the Mn(III) site, as is usual for the salen-type Schiff base complexes. In complex **1**, the formate ion axially coordinates to the metal centre. On the other hand, the nitrite ion present in the reaction mixture bridges through $\mu-1\kappa O:2\kappa O'$ mode in **2** and terminally coordinates through an oxygen atom in **3** to the Mn(III) centre (Scheme 2).

Besides elemental analysis, all the complexes were initially characterized by IR spectra. All three complexes exhibit a sharp band due to azomethine $\nu(C=N)$ at 1590, 1612 and 1589 cm^{-1} , respectively. For **1**, the strong band at 1537 cm^{-1} is likely to be due to the antisymmetric and the band at 1328 cm^{-1} to the symmetric stretching modes for the formate [24]. Bands due to $\nu_s(NO_2)$ and $\nu_{as}(NO_2)$ are observed at 1295, 1213 cm^{-1} (for **2**) and 1313, 1234 cm^{-1} (for **3**) as reported earlier for O-coordinated nitrite [30]. One additional band corresponding to $\nu(H_2O)$ is observed at 3487 and 3395 cm^{-1} for **1** and **2**, respectively. UV-vis spectra of these complexes in acetonitrile solvent show a broad band at 396 (for **1**), 388 (for **2**) and 397 nm (for **3**) corresponding to ligand to metal charge transfer [24,31].

3.2. Electrospray ionization mass spectral study

The electrospray ionization mass (ESI-MS positive) spectrum of **1–3** was recorded in acetonitrile solvent to rationalize the composition of the complex in solution state. The spectrum of **1** shows base peak at $m/z=349$ (100%) which is well assignable to the



Scheme 2. Complexes 1–3.

mononuclear species $[MnL^1]^+$. Another peak at $m/z=436$ indicates the presence of mononuclear species $[MnL^1(OOCH)(CH_3CN)H]^+$ (SI Fig. S5). The spectrum of **2** shows base peak at $m/z=279$ (100%) which is well assignable to the ligand species $[H_3L^2]^+$. Two peaks at $m/z=335$, 413 are due to the mononuclear species $[(MnL^2)]^+$ and $[(MnL^2)(CH_3CN)_2]^+$, respectively. Two other peaks at $m/z=854$, 885 can be assigned to the dinuclear species $[Mn_2(L^2)_2(NO_2)_3Na_2]^+$ and $[Mn_2(L^2)_2(NO_2)_2(CH_3CN)_3H]^+$, respectively. (SI Fig. S6) The spectrum of **3** shows a base peak at $m/z=349$ (100%) which fits well with the mononuclear species $[(MnL^1)]^+$. Four other peaks at $m/z=733$, 743, 813 and 802 are probably due to the presence of $[(MnL^1)_2Cl]^+$, $[(MnL^1)_2NO_2]^+$, $[(MnL^1)_2(NO_2)Cl]Na^+$ and $[(MnL^1)_2(NO_2)_2]Na^+$ species, respectively in the solution state (SI Fig. S7).

We have recorded ESI-MS spectra of a 1:100 mixture of complex **2** and 3,5-DTBC in acetonitrile solvent, to gain an insight of this oxidation reaction in solution state. The spectrum (SI Fig. S8) exhibits a base peak at $m/z=243$ (100%) corresponding to the quinone sodium aggregate $[3,5-DTBO-Na]^+$. The peak at $m/z=774$ corroborates the formation of $[Mn_2L_2^2O_2(CH_3CN)_2]$ via a Mn– O_2 species

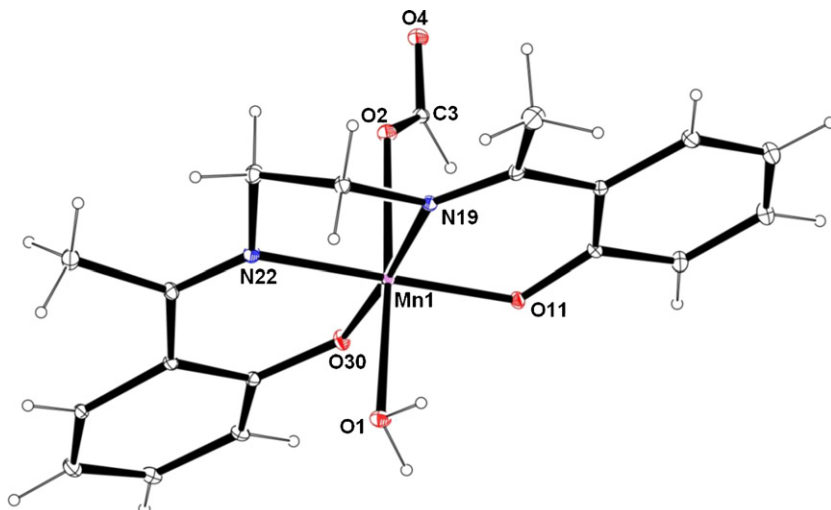


Fig. 1. The structure of **1** with ellipsoids at 30% probability.

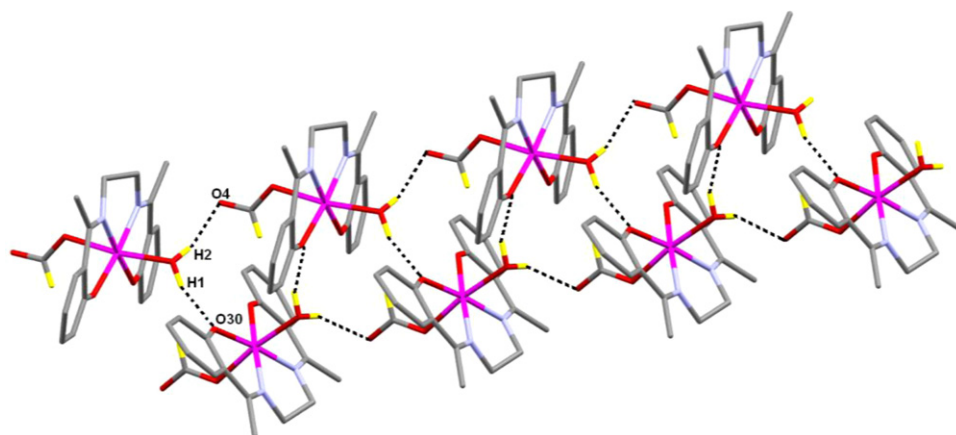


Fig. 2. Hydrogen bonded polymeric structure of **1**; hydrogen atoms except H1, H2, and H3 have been excluded for clarity.

as an intermediate [32]. Another peak at $m/z=631$ can be assigned to the mononuclear species $[\text{MnL}^2\text{O}_2(3,5\text{-DTBSQ})(\text{CH}_3\text{CN})]$.

3.3. Description of structures

The monomeric structure of **1** is shown in Fig. 1 together with the atomic numbering scheme in the coordination sphere. Here the ligand contains an ethylene link between the two nitrogen atoms N(19) and N(22). The metal has a six-coordinate octahedral environment being bonded to the four donor atoms of ligand L^1 in the equatorial plane and one water molecule and a formate anion in axial positions. The four donor atoms in the equatorial plane show a r.m.s. deviations of 0.045 Å with the metal atom 0.021(2) Å from the plane. The two phenyl rings in the ligand intersect the equatorial plane by angles of 17.8(2) and 16.0(2) with an angle of 4.2(2) between them. Bond lengths in the equatorial plane are Mn(1)–O(11) 1.847(3) Å, Mn(1)–O(31) 1.890(3) Å, Mn(1)–N(19) 1.987(4) Å, Mn(1)–N(23) 1.987(4) Å and in axial positions Mn(1)–O(1) 2.265(3) Å, Mn(1)–O(2) 2.195(3) Å (Table ST2). The two hydrogen atoms H(1) and H(2) on the water molecule form donor intermolecular hydrogen bonds to the phenoxido oxygen O(30) ($3/2-x, y+1/2, z$) and the non-coordinated oxygen atom of formate, O(4) ($x, y+1, z$) with dimensions O(1)⋯O 2.944(5), 2.684(5) Å; O(1)–H⋯O 148, 132° and H⋯O 2.17, 2.01 Å, respectively to result in a 1D chain along the b -axis (Fig. 2).

The structure of **2** contains discrete $[\text{MnL}^2(\text{OH}_2)_2]^+$ cations and $[\text{Mn}_2\text{L}_2^2(\text{NO}_2)_3]^-$ anions as shown in Figs. 3 and 4, respectively. Here the ligand contains three methylene groups between the two nitrogen atoms N(19) and N(23) rather than the two methylene groups that are found in **1**. The structure of the cation $[\text{MnL}^2(\text{OH}_2)_2]^+$ the metal in a six-coordinate octahedral environment with the metal bonded to the four donor atoms

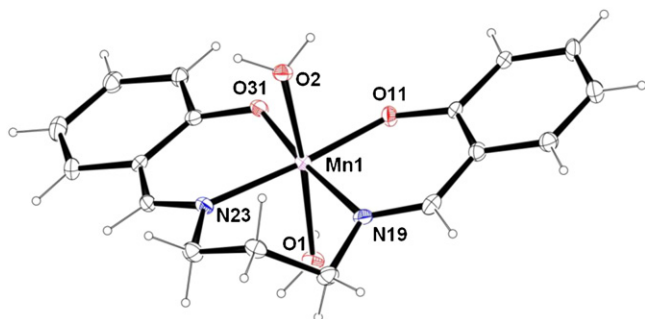


Fig. 3. The structure of the $[\text{Mn}(\text{L}^2)(\text{OH}_2)_2]^+$ cation in **2** with ellipsoids at 30% probability.

of the ligand in an equatorial plane and two water molecules in axial positions. The four donor atoms N(19), N(23), O(11), O(31) are planar with a r.m.s. deviation of 0.018 Å with the metal 0.002(2) Å from the plane. Bond lengths in the equatorial plane are Mn(1)–O(11) 1.882(3), Mn(1)–O(31) 1.857(4), Mn(1)–N(19) 2.017(5), Mn(1)–N(23) 2.040(4) Å and in axial positions Mn(1)–O(1) 2.218(4), Mn(1)–O(2) 2.283(4) Å (Table ST2). The angle between the two phenyl rings is 4.6(3) with the two rings intersecting the equatorial planes at angles of 13.0(2) and 13.2(2), respectively. Thus the conformation of the cation is similar to that found in **1**. The structure of the anion $[\text{Mn}_2\text{L}_2^2(\text{NO}_2)_3]^-$ shows two metal atoms Mn(2) and Mn(3) in similar octahedral environments bonding to the ligand L^2 with four donor atoms N(49), N(53), O(41), O(61) for Mn(2) and N(79), N(83), O(71), O(91) for Mn(3) in the equatorial plane. In the axial positions of each metal atom there are two nitrite anions, one terminal and one bridging. The two equatorial planes show r.m.s. deviations of 0.079, 0.035 Å with the metal atoms 0.043(2), 0.042(2) Å from the plane. In the equatorial plane Mn–N distances are in the range 2.006(4) to 2.029(4) Å and Mn–O distances are in the range 1.879(3) to 1.891(3) Å. Distances in axial

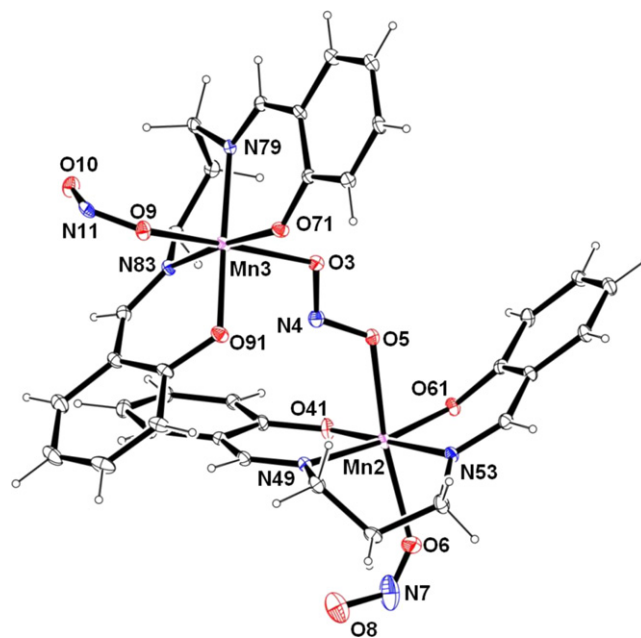


Fig. 4. The structure of the $[\text{Mn}_2(\text{NO}_2)_3\text{L}_2^2]^-$ anion in **2** with ellipsoids at 30% probability. The structure is disordered with terminal nitrite O9, N11, O10 and chloride (not shown) having refined occupation factors of 0.62(1), and 0.38(1), respectively.

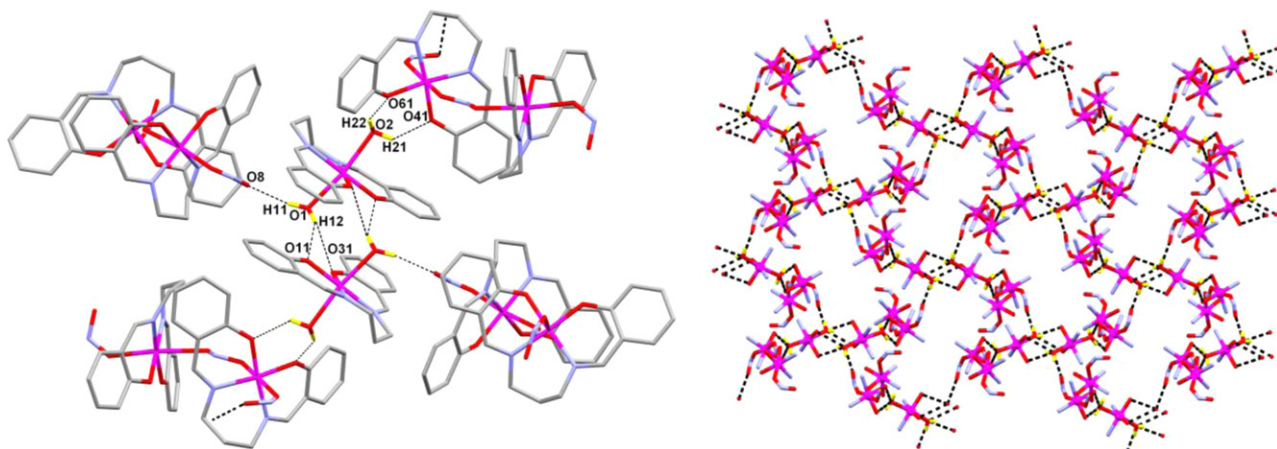


Fig. 5. Hydrogen bonded polymeric structure of **2**; hydrogen atoms, except those of the water molecules, namely H11, H12, H21, and H22, have been excluded for clarity.

positions are Mn(2)–O(6) 2.252(5), Mn(3)–O(9) 2.121(7) Å to terminal nitrites and Mn(2)–O(5) 2.236(4), Mn(3)–O(3) 2.308(4) Å to bridging nitrites. In the anion, the two ML^2 moieties show different conformations to those found in the cation and in **1**. Thus around Mn(2) the two phenyl rings intersect at $44.1(2)^\circ$ with the rings intersecting the equatorial plane at $12.4(3)$ and $32.5(2)$. Comparable angles for the ligand around Mn(3) are $2.7(3)$, $30.9(2)$, and $30.9(2)$. The two equatorial planes intersect at $62.3(1)$.

The two water molecules in the cation form four donor intermolecular hydrogen bonds (Fig. 5). From O(1) the hydrogen atom H(11) forms a hydrogen bond to an oxygen atom O(8) of nitrite ($x-1, -y+1/2, z+1/2$) with dimensions $O \cdots O$ 2.869(8) Å, $O-H \cdots O$ 169° and $H \cdots O$ 2.03 Å. The other hydrogen H(12) forms bifurcated hydrogen bonds to phenoxido oxygens O(11) ($-x, -y, 2-z$) and O(31) ($-x, -y, 2-z$) with dimensions $O \cdots O$ 2.957(5), 3.040(5) Å, $O-H \cdots O$ $149, 120^\circ$ and $H \cdots O$ 2.22, 2.54 Å, respectively. From O(2) the two hydrogen atoms H(21) and H(22) form hydrogen bonds to O(41) ($1-x, 1-y, 1-z$) and O(61) ($1-x, 1-y, 1-z$), respectively with dimensions $O \cdots O$ 2.838(5), 2.929(5) Å, $O-H \cdots O$ $130, 146, H \cdots O$ 2.22, 2.17 Å, thus forming a 2D supramolecular network.

The structure of **3**, a di-phenoxido bridged centrosymmetric dimer, is shown in Fig. 6. Here the metal atoms are bonded to the four donor atoms of the ligand in an equatorial plane with

the axial sites consisting of an anion, disordered between nitrite and chloride, and an oxygen atom of a second ligand. Bond lengths in the equatorial plane are Mn(1)–O(11) 1.854(9) Å, Mn(1)–O(30) 1.885(8) Å, Mn(1)–N(19) 2.014(10) Å, Mn(1)–N(22) 2.001(11) Å with axial bonds Mn(1)–O(30)' ($' = -x, 1-y, -z$) 2.520(9) Å and Mn(1)–Cl(1) 2.503(12) Å or Mn(1)–O(3) 2.09(4) Å (Table S2). The donor atoms in the equatorial plane show an r.m.s. deviation of 0.060 Å with the metal 0.184(6) Å from the plane in the direction of the disordered anion. The two phenyl rings intersect at $20.9(8)$ and intersect the equatorial plane at angles at $8.2(8)$ and $28.0(6)$.

3.4. Kinetics of the oxidation of 3,5-di-tert-butylcatechol

The catecholase activity of complexes **1–3** was studied using 3,5-DTBC as a convenient model substrate [33], in air saturated acetonitrile solvent at room temperature (25°C). For this purpose, a 1×10^{-5} M solution of these complexes was treated with 1×10^{-3} M (100 equiv.) of 3,5-DTBC and the course of the reaction was followed by recording the UV-vis spectra of the mixture at an interval of 5 min. After addition of substrate 3,5-DTBC to the solutions of the catalysts **1–3**, a gradual increase of the band corresponding to 3,5-DTBQ was observed at 400 nm (Fig. 7 for complex **2** and Figs. S1 and S3 in supporting information for complexes **1** and **3**, respectively).

The kinetics of oxidation of 3,5-DTBC were determined by the method of initial rates and involved monitoring the growth of

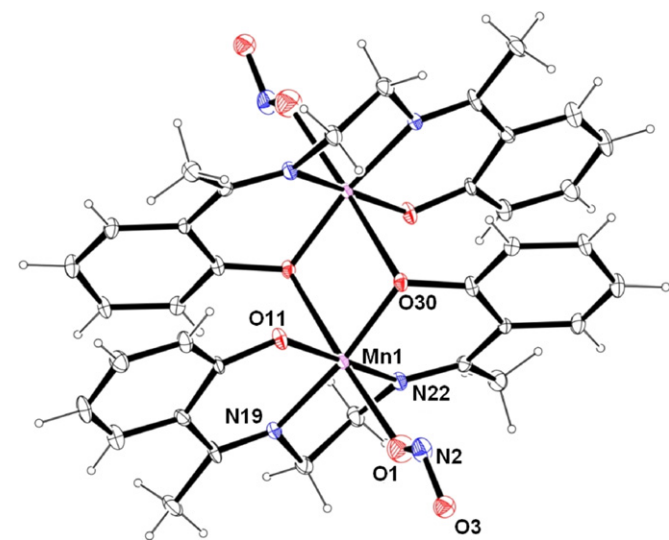


Fig. 6. The structure of the centrosymmetric dimer $[Mn_2L_2(NO_2)_2]$ in **3** with ellipsoids at 30% probability. The terminal nitrite O1, N2, O3 is disordered at 50% with a chloride (not shown).

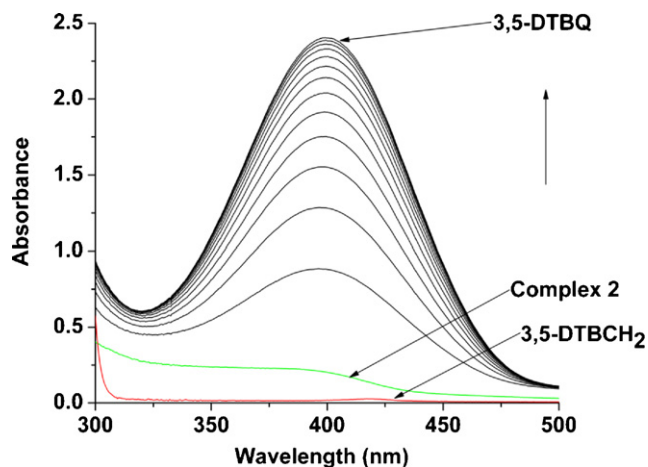


Fig. 7. Increase of quinone band at 400 nm after addition of 100 fold 3,5-DTBC to complex **2** (10^{-5} M) in acetonitrile solvent. The spectra were recorded at an interval of 5 min.

Table 1
Kinetic parameters for oxidation of 3, 5-DTBC catalyzed by various complexes.

Complex	V_{\max} (M min ⁻¹)	Std. error	K_M (M)	Std. error	K_{cat} (h ⁻¹)
1	1.606×10^{-4}	1.374×10^{-5}	5.501×10^{-4}	1.506×10^{-6}	936.64
2	6.089×10^{-5}	4.380×10^{-6}	6.408×10^{-4}	1.081×10^{-6}	365.34
3	2.388×10^{-4}	9.395×10^{-6}	4.917×10^{-3}	3.803×10^{-5}	1432.74

the quinone band at 400 nm as a function of time. To determine the dependence of the rates on the substrate concentration and various kinetic parameters, solutions of **1–3** were treated with different concentrations of 3,5-DTBC (from 10 to 100 equiv.) under aerobic conditions. The data were taken at an interval of 30 s and the conversion was measured up to 10 min in each case. From these data the rate of the catechol oxidation reaction with varying substrate concentration was found out. At low concentrations of 3,5-DTBC a first-order dependence of the substrate concentration was observed. At higher concentrations, saturation kinetics was found for all compounds. The rate constant versus concentration of substrate data was then analyzed on the basis of the Michaelis–Menten approach of enzymatic kinetics to obtain the Lineweaver–Burk (double reciprocal) plot as well as the values of the various kinetic parameters V_{\max} , K_M , and K_{cat} . Observed rate vs. [substrate] plot and the Lineweaver–Burk plot for complex **2** are shown in Fig. 8. Similar plots for **1** and **3** are given in the supporting information (SI Figs. S2 and S4, respectively). The kinetic parameters for all cases are listed in Table 1. We have also carried out kinetic experiments by varying the catalyst concentration, keeping the substrate concentration at 10^{-3} M, and found a first order rate dependence for all the three catalysts **1–3** (Fig. 9).

The enzyme catechol oxidase consists of a hydroxobridged dicopper(II) center and consequently mono or dinuclear copper complexes are extensively studied as model complexes to examine catecholase activity. It has been found that structural features and electrochemical properties are important factors in determining the catalytic activity of these complexes [34]. The mechanistic course of catechol oxidation reaction catalyzed by copper(II) complexes has been extensively studied [35,36]. But up to now there has been only limited study of plausible mechanisms of this reaction using manganese(II/III) complexes as catalyst [37–39]. However, there is some ambiguity regarding the participation of metal centre in the catechol to quinone oxidation process [17]. In order to understand whether the redox participation of the metal center is responsible for the catecholase activity established for our Mn(III) complexes, we have performed an EPR study at 77 K selecting complex **2** as the catalyst. For this, we have prepared a 1:100 mixture

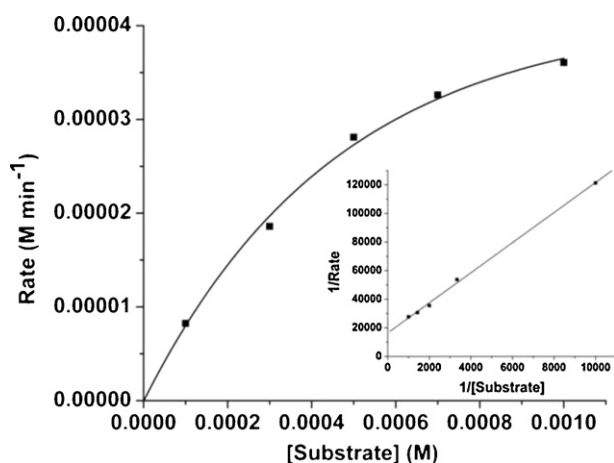


Fig. 8. Plot of rate vs. substrate concentration for complex **2**. Inset shows Lineweaver–Burk plot.

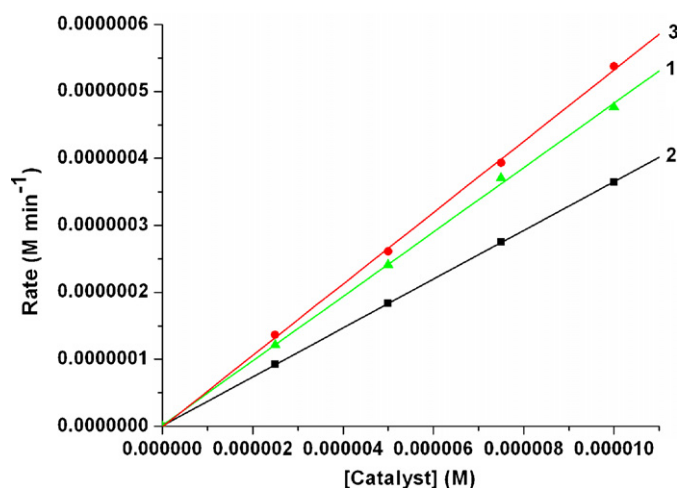


Fig. 9. Plot of rate vs. catalyst concentration for the oxidation reaction of 3,5-DTBC (10^{-3} M) catalyzed by the complexes **1–3** in acetonitrile solvent.

of complex **2** and 3,5-DTBC (10^{-1} M) in acetonitrile solvent and recorded the EPR spectra within 2 min of mixing. A characteristic six line EPR spectrum (Fig. 10) corroborates the generation of Mn(II) species from Mn(III) species during the catalytic oxidation of 3,5-DTBC to 3,5-DTBQ in presence of aerial oxygen. To detect the percentage of formation of Mn(II) species during this oxidation reaction, we have utilized the spin-quantitation method [40]. In this method the double-integrated value of EPR spectra (first-derivative signal) of the experimental sample is usually compared with a standardized species whose spin content and concentration is known. For this purpose we have recorded the EPR spectra of a 1:100 mixture of complex **2** (concentration of Mn(III) is 3.0×10^{-3} M) and 3,5-DTBC and compared the EPR peak intensity with that obtained from a standard Mn(II) complex of 10^{-3} M concentration (Fig. S9). From the double integral values of these two spectra in the range 3000–3600 G (Fig. S10) we have calculated the concentration of

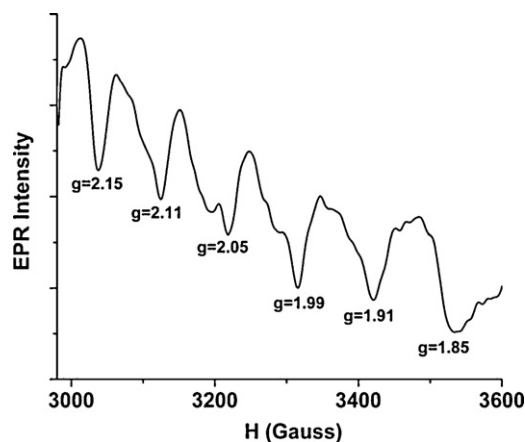
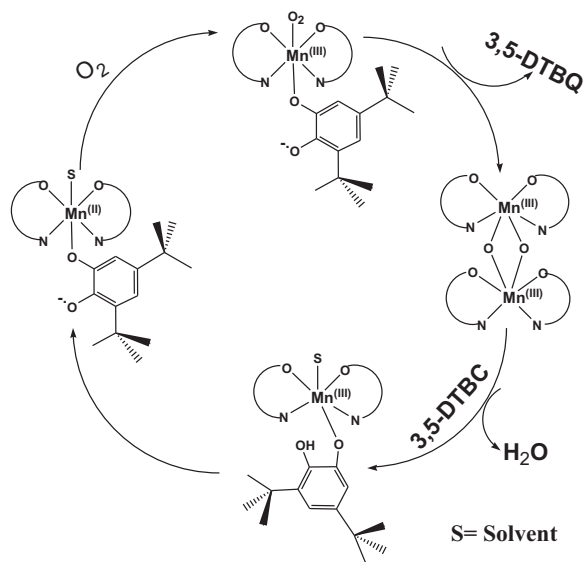


Fig. 10. EPR spectrum of a 1:100 mixture of complex **2** and 3,5-DTBC (10^{-1} M) in acetonitrile at 77 K. Center field: 3000.000 G; sweep width: 2.5×100 mT; microwave frequency: 9126.324 MHz; mod frequency: 100.00 KHz; mod width: 1.0×0.1 mT; time const.: 0.03.



Scheme 3. Formation of different intermediate species during the course of catechol oxidation.

Mn(II) species within the reaction mixture to be 2.106×10^{-3} M i.e. conversion of Mn(III) to Mn(II) is 70.20%.

The results obtained from ESI-MS indicate that the reaction is initiated by dioxygen binding to the metal centre of **2**, thus forming bis(μ -oxo)dimanganese(III,III) as an intermediate. This dinuclear complex reacts with 3,5-DTBC to produce the $[L^2Mn(O_2)-3,5-DTBSQ]$ adduct (Scheme 3) and finally 3,5-DTBQ is eliminated.

The turnover rate of complex **1** is comparable to those values reported for mononuclear Mn(III).^[10,16] The presence of one labile water molecule in the coordination sphere of Mn(III) enhances the rate of catechol oxidation. The cationic part of complex **2** also contains two labile water molecules, but the lower activity of this complex may be attributed to the fact that the anionic part contains bridging nitrite, which is a poorer leaving group ($Mn(3)-O(3) = 2.308 \text{ \AA}$ and $Mn(2)-O(5) = 2.236 \text{ \AA}$). Between **2** and **3**, probably the M–M distance (5.971 \AA for **2** and 3.458 \AA for **3**) is the deciding factor for the rate of catecholase activity. Besides, in **3**, two Mn(III) centers are connected through a weak phenoxido bridge ($Mn(1)-O(30') = 2.520 \text{ \AA}$) which may be responsible for higher catalytic activity.

4. Conclusions

In this paper we present three Mn(III) complexes of salen-type di-Schiff base ligands that are structurally related to the proposed active site of catechol oxidase enzyme. These three complexes (**1–3**) exhibit high catalytic activity for the oxidation of 3,5-di-tert-butylcatechol to 3,5-di-tertbutylquinone. They belong to the class of synthetic catechol oxidase model compounds showing first-order rate dependence at lower substrate concentration and saturation kinetics at higher substrate concentrations. The ESI-MS positive spectrum of **2** in the presence of 3,5-DTBC indicates the formation of bis(μ -oxo)dimanganese(III,III) as an intermediate. The characteristic six line EPR spectra of the complex in the presence of 3,5-DTBC is evidence for the formation of manganese(II)-semiquinonate as an intermediate species during the catalytic oxidation of 3,5-DTBC. Therefore, the present study contributes to the development of biomimetic manganese(III) complexes that can catalyze the reaction performed by catechol oxidases.

Electronic supplementary data

Enzyme kinetics data for **1** and **3**, ESI-MS spectra, EPR spectra. Crystal data, bond lengths and bond angles in the metal coordination spheres of **1–3**. CCDC-872032 (for **1**), -872033 (for **2**), -872034 (for **3**) contain the supplementary crystallographic data for this paper. These data can be obtained free of charge from The Cambridge Crystallographic Data Centre via www.ccdc.cam.ac.uk/data_request/cif.

Acknowledgments

We thank EPSRC and the University of Reading for funds for the X-Calibur system for data of **1** and **2**. We thank DST-FIST, India-funded Single Crystal Diffractometer Facility at the Department of Chemistry, University of Calcutta, Kolkata, India for data of **3**. We are also thankful to UGC for Junior Research Fellowship to P.S (UGC/20/Jr. Fellow (Sc) dated 10.01.2011).

Appendix A. Supplementary data

Supplementary data associated with this article can be found, in the online version, at <http://dx.doi.org/10.1016/j.molcata.2012.08.024>

References

- [1] L.I. Simándi, *Catalytic Activation of Dioxygen by Metal Complexes*, Kluwer, Dordrecht, 1992.
- [2] E.I. Solomon, U.M. Sundaram, T.E. Machonkin, *Chem. Rev.* 96 (1996) 2563.
- [3] E.B. Meunier, *Biomimetic Oxidations Catalyzed by Transition Metal Complexes*, Imperial College Press, London, 2000.
- [4] J. Reedijk, *Bioinorganic Catalysis*, Dekker, New York, 1993.
- [5] M. Costas, M.P. Mehn, M.P. Jensen, L. Que Jr., *Chem. Rev.* 104 (2004) 939.
- [6] E.A. Lewis, W.B. Tolman, *Chem. Rev.* 104 (2004) 1047.
- [7] R. Hage, A. Lienke, *Angew. Chem.* 118 (2006) 212.
- [8] P. Gentschev, N. Möller, B. Krebs, *Inorg. Chim. Acta* 442 (2000) 300.
- [9] M.G. Alvarez, G. Alzuete, J. Borras, S.G. Granda, J.M.M. Bernardo, *J. Inorg. Biochem.* 96 (2003) 443.
- [10] K. Selmececi, M. Réglie, M. Giorgi, G. Speier, *Coord. Chem. Rev.* 245 (2003) 191.
- [11] I.A. Koval, P. Gamez, C. Belle, K. Selmececi, J. Reedijk, *Chem. Soc. Rev.* 35 (2006) 814.
- [12] A. Guha, K.S. Banu, A. Banerjee, T. Ghosh, S. Bhattacharya, E. Zangrando, D. Das, *J. Mol. Catal. A* 338 (2011) 51.
- [13] J. Kaizer, G. Baráth, R. Csonka, G. Speier, L. Korecz, A. Rockenbauer, L. Párkañyi, *J. Inorg. Biochem.* 102 (2008) 773.
- [14] J. Kaizer, R. Csonka, G. Baráth, G. Speier, *Trans. Met. Chem.* 32 (2007) 1047.
- [15] A. Majumder, S. Goswami, S.R. Batten, M.S.E. Fallah, J. Ribas, S. Mitra, *Inorg. Chim. Acta* 359 (2006) 2375.
- [16] K.S. Banu, T. Chattopadhyay, A. Banerjee, M. Mukherjee, A.S. Bhattacharya, G.K. Patra, E. Zangrando, D. Das, *Dalton Trans.* (2009) 8755.
- [17] S. Mukherjee, T. Weyhermüller, E. Bothe, K. Wieghardt, P. Chaudhuri, *Dalton Trans.* (2004) 3842.
- [18] G. Blay, I. Fernández, J.R. Pedro, R. Ruiz, T.T. Sánchez, E. Pardo, F. Lloret, M.C. Muñoz, *J. Mol. Catal. A* 250 (2006) 20.
- [19] J.J.R. Frausto da Silva, R.J.P. Williams, *The Biological Chemistry of the Elements*, Clarendon Press, Oxford, 1991, p. 370.
- [20] V.L. Pecoraro (Ed.), *Manganese Redox Enzymes*, VCH, New York, 1992.
- [21] H.L. Shyu, H.H. Wei, Y. Wang, *Inorg. Chim. Acta* 290 (1999) 8.
- [22] Z. Lü, M. Yuan, F. Pan, S. Gao, D. Zhang, D. Zhu, *Inorg. Chem.* 45 (2006) 3538.
- [23] H. Miyasaka, R. Clérac, W. Wernsdorfer, L. Lecren, C. Bonhomme, K.I. Sugiura, M. Yamashita, *Angew. Chem.* 116 (2004) 2861.
- [24] P. Kar, R. Biswas, M.G.B. Drew, Y. Ida, T. Ishida, A. Ghosh, *Dalton Trans.* (2011) 3295.
- [25] M. Hariharan, F.L. Urbach, *Inorg. Chem.* 8 (1969) 556.
- [26] CrysAlis, Oxford Diffraction Ltd., Abingdon, U.K., 2006.
- [27] G.M. Sheldrick, *Acta Cryst. A* 64 (2008) 112.
- [28] ABSPACK, Oxford Diffraction Ltd., Oxford, U.K., 2005.
- [29] SAINT, Version 6.02; SADABS, Version 2.03, Bruker AXS, Inc., Madison, WI, 2002.
- [30] N. Lehnert, U. Cornelissen, F. Neese, T. Ono, Y. Noguchi, K. Okamoto, K. Fujisawa, *Inorg. Chem.* 46 (2007) 3916.
- [31] P. Kar, P.M. Guha, M.G.B. Drew, T. Ishida, A. Ghosh, *Eur. J. Inorg. Chem.* (2011) 2075.
- [32] H. Komatsuzaki, Y. Nagasu, K. Suzuki, T. Shibasaki, M. Satoh, F. Ebina, S. Hikichi, M. Akita, Y. Moro-oka, *J. Chem. Soc., Dalton Trans.* (1998) 511.
- [33] R. Than, A.A. Feldmann, B. Krebs, *Coord. Chem. Rev.* 182 (1999) 211.
- [34] M.U. Triller, D. Pursche, W.Y. Hsieh, V.L. Pecoraro, A. Rompel, B. Krebs, *Inorg. Chem.* 42 (2003) 6274.

- [35] F. Zippel, F. Ahlers, R. Werner, W. Haase, H.F. Nolting, B. Krebs, *Inorg. Chem.* 35 (1996) 3409.
- [36] I.A. Koval, K. Selmeczi, C. Belle, C. Philouze, E.S. Aman, I.G. Luneau, A.M. Schuitema, M. Vliet, P. Gamez, O. Roubeau, M. Lüken, B. Krebs, M. Lutz, A.L. Spek, J.-L. Pierre, J. Reedijk, *Chem. Eur. J.* 12 (2006) 6138.
- [37] Y. Hitomi, A. Ando, H. Matsui, T. Ito, T. Tanaka, S. Ogo, T. Funabiki, *Inorg. Chem.* 44 (2005) 3473.
- [38] N. Shaikh, A. Panja, P. Banerjee, M. Ali, *Trans. Met. Chem.* 28 (2003) 871.
- [39] I.C. Szgyártó, L.I. Simándi, L. Párkányi, L. Korecz, G. Schlosser, *Inorg. Chem.* 45 (2006) 7480.
- [40] D.A. Svistunenko, M.A. Sharpe, P. Nicholls, M.T. Wilson, C.E. Cooper, *J. Magn. Reson.* 142 (2000) 266.